



Computational Materials Science for Materials under Extremes

Alfredo Caro - Los Alamos National Laboratory USA

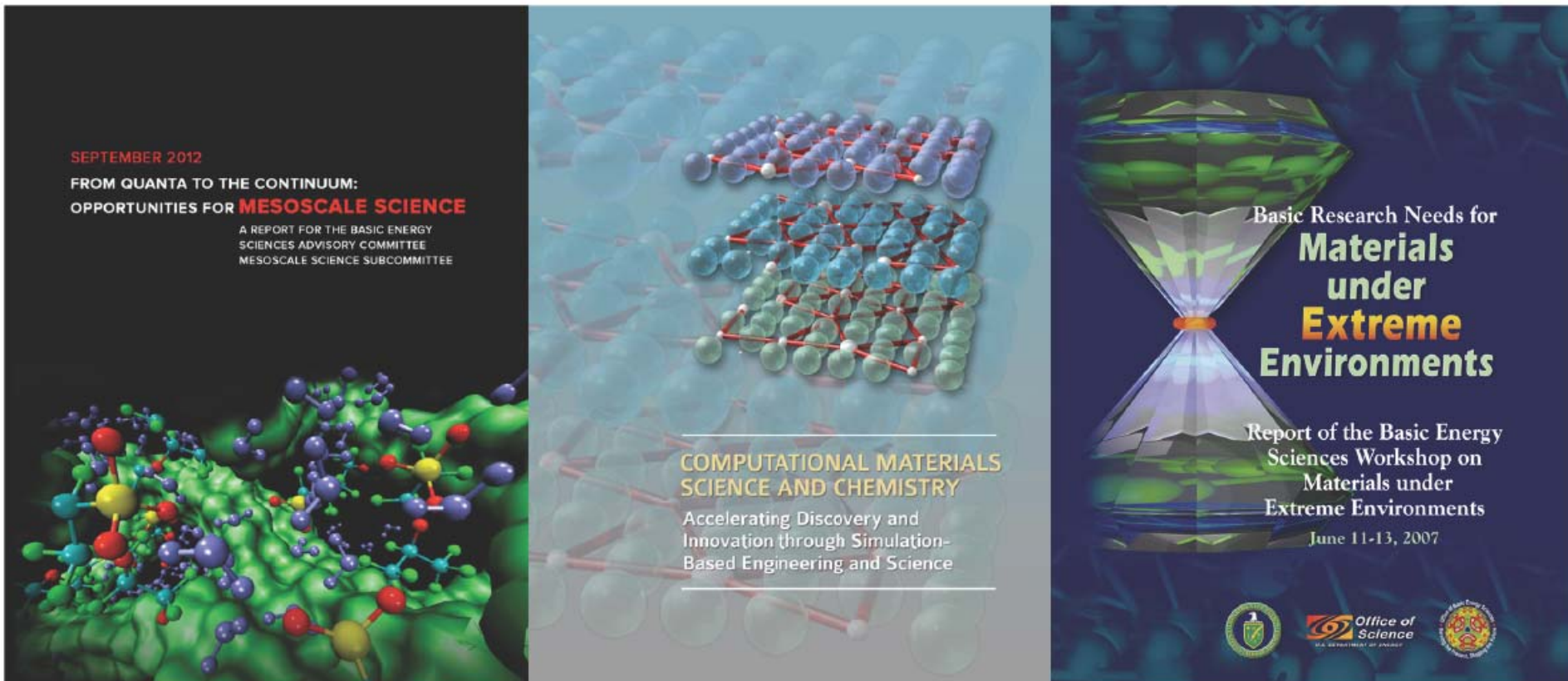
Primer encuentro virtual de la red CompuMat

May 23 2014

How science directions are chosen:

<http://science.energy.gov/bes/news-and-resources/reports/>

Computational materials science, particularly at the mesoscale, is a focus



Energy Frontier Research Center

for Materials under Irradiation and Mechanical Extremes

<http://science.energy.gov/bes/efrc/>



Institutions:
LANL, MIT, UIUC, CMU, UNL

CMIME Org Chart
<http://cmime.lanl.gov>

Amit Misra, Director
Irene J. Beyerlein, Co-Director
Linda Chavez (admin)

Scientific Advisory Committee
Michael I. Baskes (Chair); William D. Nix;
John P. Hirth; G. Robert Odette;
Adrian Sutton; Francois Willaime.

Irradiation extremes thrust		Mechanical extremes thrust	
Metals	Oxides	Severe Plastic Deformation	High Strain Rates
Staff scientists / faculty		Staff scientists / faculty	
Michael J. Demkowicz (MIT), lead	Bias P. Uberuaga, lead	Irene J. Beyerlein, lead (theory)	Timothy C. Germann, lead
J. Alfredo Caro, PI	Steve M. Valone, Co-I	Nathan Mara, lead (experiments)	Ellen Cerreta, PI
Amit Misra, PI	*Arthur F. Voter, Co-I	Pascal Bellon (UIUC), PI	Rusty Gray, Co-I
*Stuart Maloy, Co-I	*Quanxi Jia, Co-I	Robert S. Averback (UIUC), Co-I	Richard G. Hoagland, consultant (Lab associate)
*Mike Nastasi (UNL), Co-I		*Tony Rollett (CMU), Co-I	
		**Jian Wang, Co-I	
	Post-docs		
Nan Li, 50%, (Misra)	**Samrat Choudhary, fellow (Uberuaga/Staneek)	**Keonwook Kang (Beyerlein)	Christian Brandl, 50%, (Germann)
Osman Anderoglu, 50%, (Maloy/Misra)	Kedarnath Kolluri, 50% (Uberuaga/Valone)	**John Carpenter (Mara)	**Ruifeng Zhang, fellow (Germann/Beyerlein)
Enrique Martinez-Seaz (Caro)	Louis Vernon, 50%, (Voter/Uberuaga)	**Shijian Zheng (Mara)	Alex Perez-Bergquist, 50%, (Cerreta)
Engang Fu, (Nastasi/ Y. Wang)	Zhenxing Bi, (Jia)	Weizhong Han (Mara/Misra/Cerreta)	
	Jeff Aguilar, (Uberuaga/Misra)		
	Graduate Students		
Liang Zhang, MIT (Demkowicz)	*Yun Xu, NMSU (Luo/Uberuaga)	Elvan Ekiz, UIUC (Bellon)	*Katrina Uychaco, UCSD (Meyers/Germann)
Abhishek Kashinath, MIT (Demkowicz)	*Helen Telilla, UNM (Atlas/Valone)	Tim Lach, UIUC (Averback)	**Benjamin Eftink, UIUC (Robertson/Mara)
		Jon LeDonne, CMU (Rollett/Mara)	
		*Thomas Nizolek, UCSB (Pollock/Mara)	

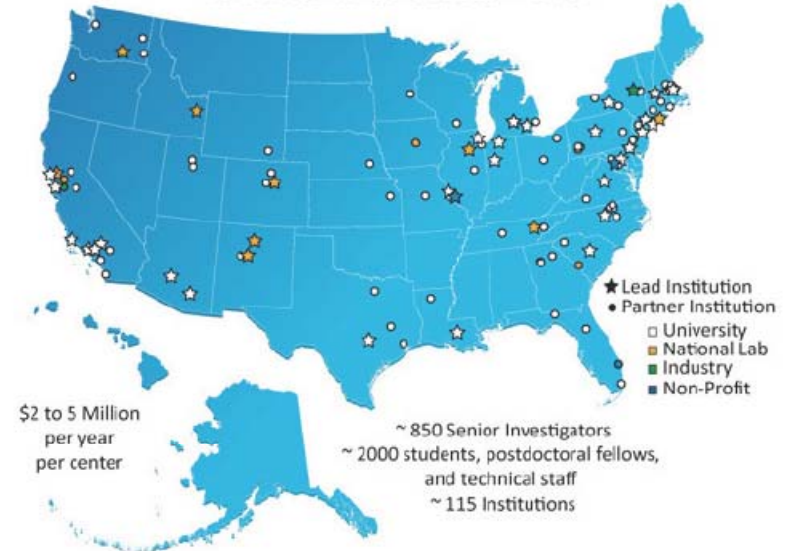
LANL Technical Staff:
Rob and Pat Dickerson (EML);
Yong Wang (IBML); J. Kevin Baldwin (PVD);
Faculty collaborators thru' LANL Institutes:
Tresa Pollock, UC-SB
Susan Atlas, UNM
Hongmei Luo, NMSU
Marc Meyers, UCSD

*GRA supported through LANL Institutes
‡ (post-doc or student support only)
** LANL/LDRD Leveraged

Former post-docs:
A. Vaitre; X-M. Bai; A. Karakuscu; Mujin Zhuo.

18 LANL staff ≈ 4 FTE
5 faculty
16 post-docs (≈ 13.5 FTE)
10 students, including 5 supported by LANL institutional resources

46 EFRCs in 35 States + D.C.



These Centers involve significant resources and many people

Our Center at LANL focuses into interfaces



Government and industry are looking into exascale computer power



TOP 500 SUPERCOMPUTER SITE

Home | Project | Features | Lists | Statistics | Contact

Search [] Go

Home / Galleries / Tianhe-2

Tianhe-2 (MilkyWay-2) - TH-IVB-FEP Cluster, Intel Xeon E5-2692 12C 2.200GHz, TH Express-2, Intel Xeon Phi 31S1P

Site: National Super Computer Center in Guangzhou
Manufacturer: NUDT
Cores: 3,120,000
Lingpack Performance (Rmax): 33,862.7 TFlop/s
Theoretical Peak (Rpeak): 54,902.4 TFlop/s
Power: 17,808.00 kW
Memory: 1,024,000 GB
Interconnect: TH Express-2
Operating System: Kylin Linux
Compiler: gcc
Math Library: Intel MKL-11.0.0
MPI: MPICH2 with a customized GLEX channel

Ranking

List	Rank	System	Vendor	Total Cores	Rmax (TFlops)	Rpeak (TFlops)	Power (kW)
11/2013	1	TH-IVB-FEP Cluster, Intel Xeon E5-2692 12C 2.200GHz, TH Express-2, Intel Xeon Phi 31S1P	NUDT	3,120,000	33,862.7	54,902.4	17,808.00
06/2013	1	TH-IVB-FEP Cluster, Intel Xeon E5-2692 12C 2.200GHz, TH Express-2, Intel Xeon Phi 31S1P	NUDT	3,120,000	33,862.7	54,902.4	17,808.00

TOP10 November 2013

- 1 Tianhe-2 (MilkyWay-2) - TH-IVB-FEP Cluster, Intel Xeon E5-2692 12C 2.200GHz, TH Express-2, Intel Xeon Phi 31S1P NUDT
- 2 Titan - Cray XK7, Opteron 6274 16C 2.200GHz, Cray Gemini Interconnect, NVIDIA K20x Cray Inc.
- 3 Sequoia - BlueGene/Q, Power BOC 16C 1.60 GHz, Custom BM
- 4 K computer, SPARC64 VIIx 2.0GHz, Tofu Interconnect Fujitsu
- 5 Mira - BlueGene/Q, Power BOC 16C 1.60GHz, Custom BM
- 6 Ple Daint - Cray XC30, Xeon E5-2670 8C 2.800GHz, Avia Interconnect, NVIDIA K20x Cray Inc.
- 7 Stampede - PowerEdge C820, Xeon E5-2680 8C 2.700GHz, Infiniband FDR, Intel Xeon Phi SE10P Dell
- 8 JUQUEEN - BlueGene/Q, Power BOC 16C 1.600GHz, Custom Interconnect BM
- 9 Vulcan - BlueGene/Q, Power BOC 16C 1.600GHz, Custom Interconnect BM

10⁶ mega M
 10⁹ giga G
 10¹² tera T
 10¹⁵ peta P
 10¹⁸ exa E

The # 1 computer today has 3 million cores and consumes 17 MW, to deliver ~ 50 PF

With this technology, 1 EF computer would need 60 million cores and 340 MW

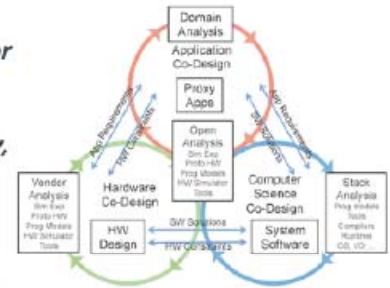
ExMatEx Overview

DoE Exascale Co-Design Center for Materials in Extreme Environments.

The objective of the Exascale Co-design Center for Materials in Extreme Environments (ExMatEx) is to establish the interrelationship among algorithms, system software, and hardware required to develop a multiphysics exascale simulation framework for modeling materials subjected to extreme mechanical and radiation environments. Such a simulation capability will play a key role in solving many of today's most pressing problems, including producing clean energy, extending nuclear reactor lifetimes, and certifying the aging nuclear stockpile.

Our goal is to establish the interrelationships between hardware, middleware (software stack), programming models and algorithms to enable a productive exascale environment for multiphysics simulations of materials in extreme mechanical and radiation environments.

We will exploit, rather than avoid, the greatly increased levels of concurrency, heterogeneity, and flop/byte ratios expected on the upcoming extreme scale platforms.



Co-design of the exascale ecosystem involves ExMatEx and other application co-design centers working in concert with hardware vendors and other computer science research activities as illustrated in the image to the right. The computer system architecture is shown to contain both the emerging hardware as well as all of the software stack required to operate the computer. The role of the application co-design center is to both introduce our evolving application requirements and workflow into the exascale ecosystem through proxy application and to evaluate these applications in the context of emerging hardware and software solutions.

Research Areas

Our research spans a broad set of topics including computer science, algorithms, and applications.



PROGRAMMING MODELS

We're engaged in the assessment and evaluation of both traditional programming languages, emerging programming paradigms, and domain specific languages.



RUNTIME SYSTEMS

Runtime system services can support "programming in the large"—coupling multiple diverse components of a dynamic multi-scale computation and orchestrating its execution on the system.

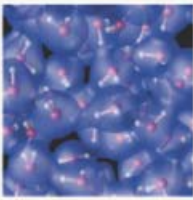
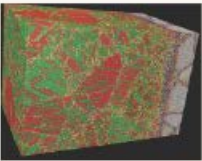
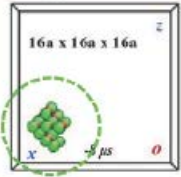



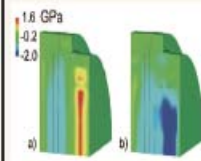


ANALYSIS, MODELING & SIMULATION

Hardware-interfacing tools combining analytical models, architectural simulation, system emulation and empirical measurements drive the co-design process.

Subjects chosen to become the equivalent to LINPACK benchmarks for the exascale era

The Motifs of Materials Application Codes

Ab-initio	MD	Long-time	Phase Field	Dislocation	Crystal	Continuum
Inter-atomic forces, EOS	Defects and interfaces, nucleation	defects and defect structures	Meso-scale multi-phase evolution	Meso-scale strength	Macro-scale material response	Macro-scale material response
						
Code: Qbox/LATTE Motif: Particles and wavefunctions, plane wave DFT, ScaLAPACK, BLACS, and custom parallel 3D FFTs Prog. Model: MPI + CUBLAS/CUDA	Code: SPaSM/ddcMD/CoMD Motif: Particles, explicit time integration, neighbor and linked lists, dynamic load balancing, parity error recovery, and <i>in situ</i> visualization Prog. Model: MPI + Threads	Code: SEAKMC Motif: Particles and defects, explicit time integration, neighbor and linked lists, and <i>in situ</i> visualization Prog. Model: MPI + Threads	Code: AMPE/GL Motif: Regular and adaptive grids, implicit time integration, real-space and spectral methods, complex order parameter Prog. Model: MPI	Code: ParaDis Motif: "segments" Regular mesh, implicit time integration, fast multipole method Prog. Model: MPI	Code: VP-FFT Motif: Regular grids, tensor arithmetic, meshless image processing, implicit time integration, 3D FFTs. Prog. Model: MPI + Threads	Code: ALE3D/LULESH Motif: Regular and irregular grids, explicit and implicit time integration. Prog. Model: MPI + Threads

Note that VP-FFT is a development of an Argentinian colleague working at LANL (R. Lebensohn)



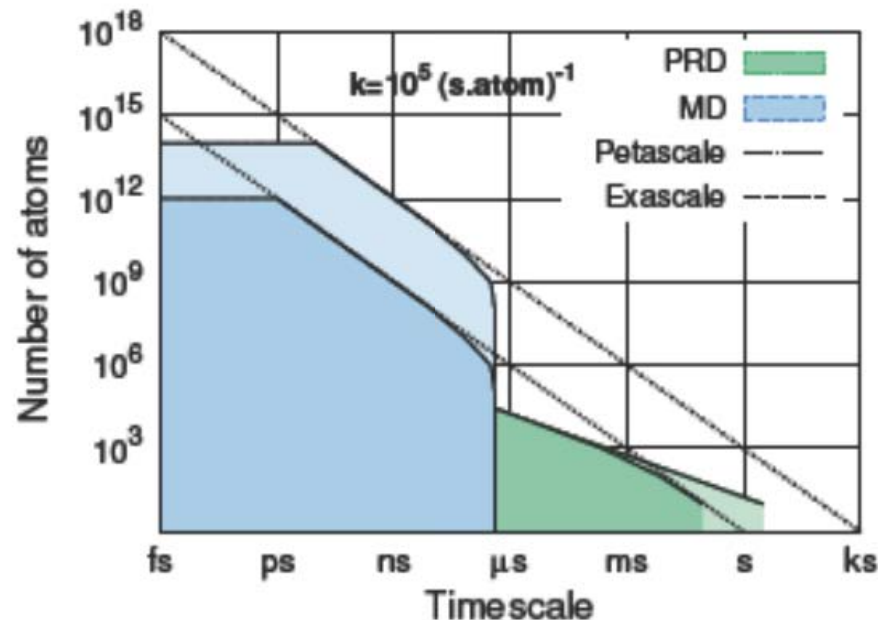
3



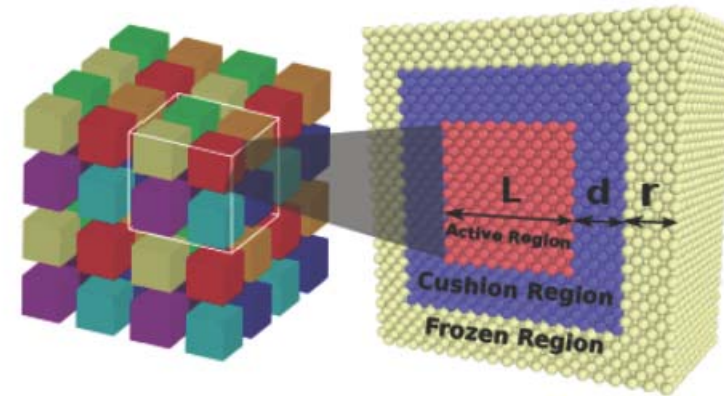
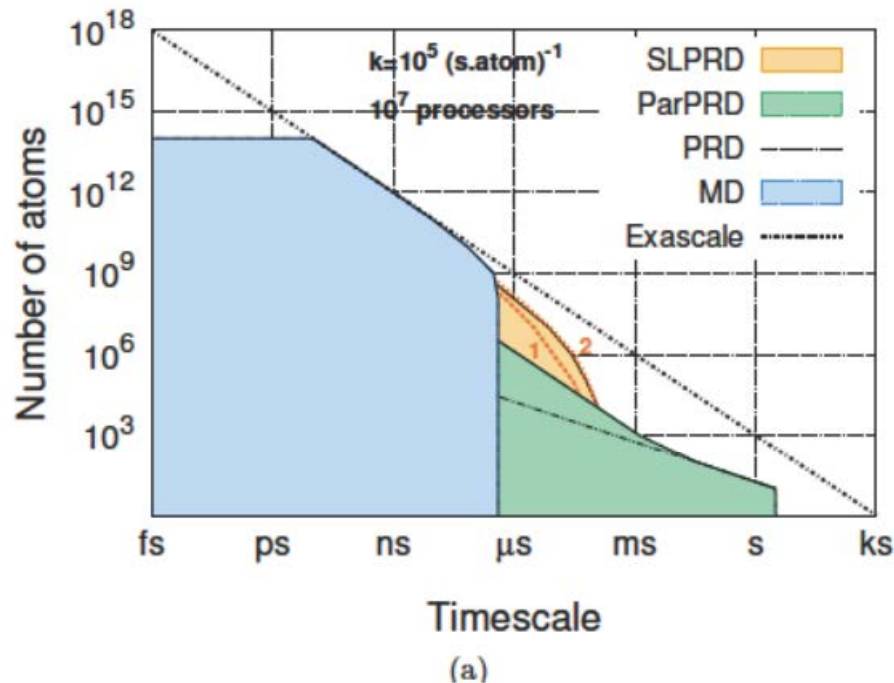
Example of exascale challenges: Sublattice parallel replica dynamics

Enrique Martínez, Blas P. Uberuaga, and Arthur F. Voter (in press)

- Exascale computing presents a challenge for the scientific community as new algorithms must be developed to take full advantage of the new computing paradigm
- Molecular dynamics and parallel replica dynamics fail to use the whole machine speedup, leaving a region in time and sample size that is unattainable with current algorithms
- Molecular dynamics (MD) algorithms are extremely efficient in parallelizing space, and therefore large atomic systems can be simulated for short times with unprecedented accuracy
- However, these traditional algorithms are not suitable for studying long-time phenomena, such as vacancy diffusion, as they become communication bound and the characteristic time for the process becomes extremely hard to attain
- Parallel replica dynamics (PRD) exploits the fact that for many physical processes the system trajectory executes transitions from state to state on time scales orders of magnitude larger than the atomic vibrations; i.e., the dynamics of the system are dominated by infrequent events.



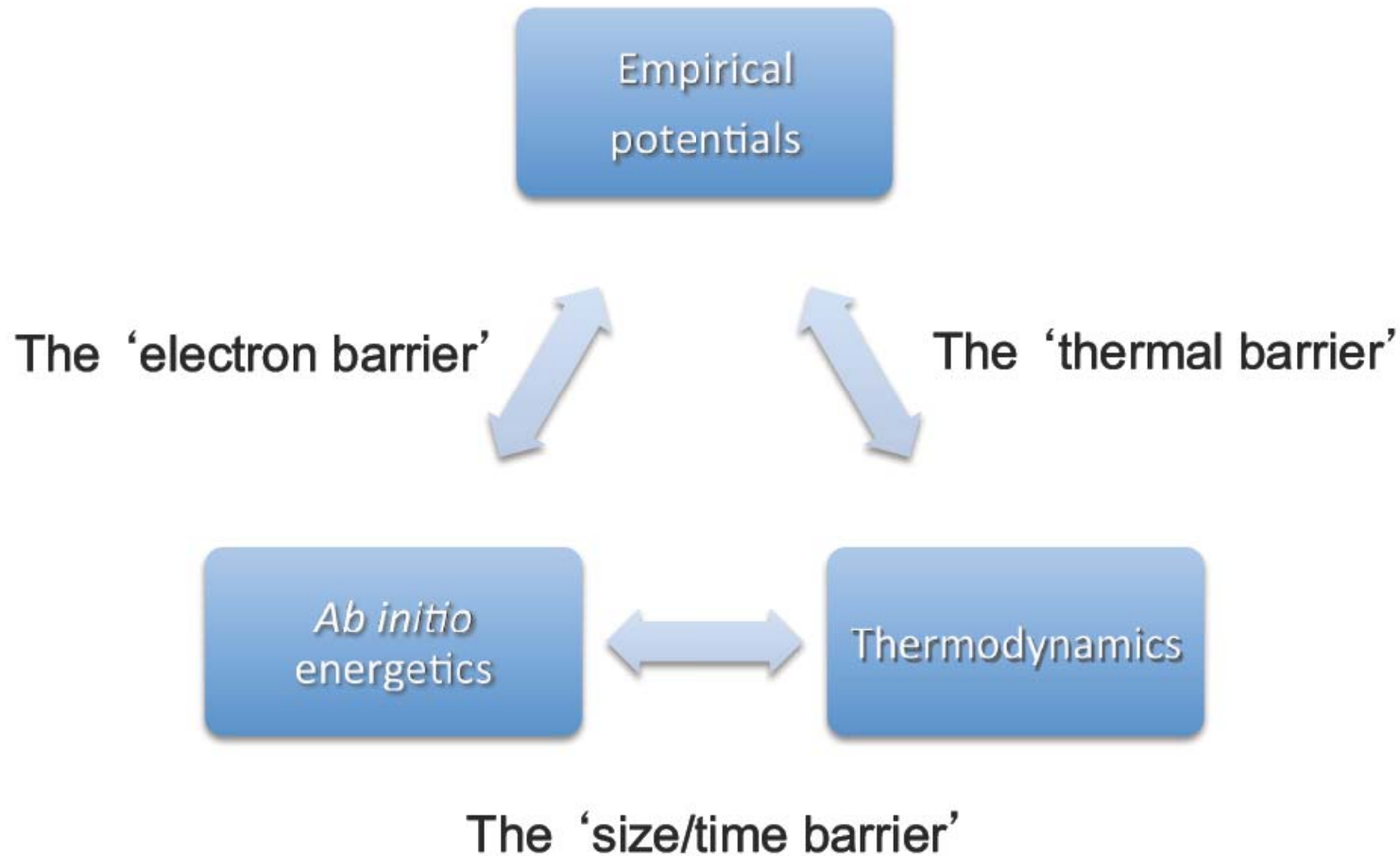
A new strategy for domain decomposition allows to fill part of the gap in the exascale triangle



Exascale triangle, assuming 10^7 processors, for the three different methods, MD (blue), ParPRD (green) and SLPRD (beige) for event rates of $k = 10^5 \text{ (s.atom)}^{-1}$

Spatial domain decomposition. To avoid boundary conflicts the domains are further divided into subdomains. Simulation cycles among the colors, performing parallel replica dynamics in each of the subdomain independently

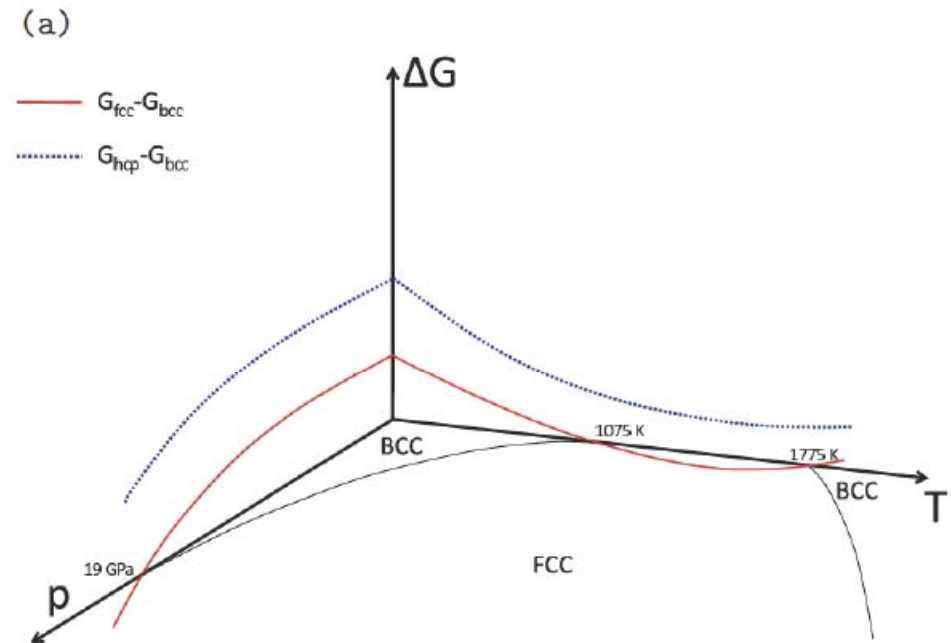
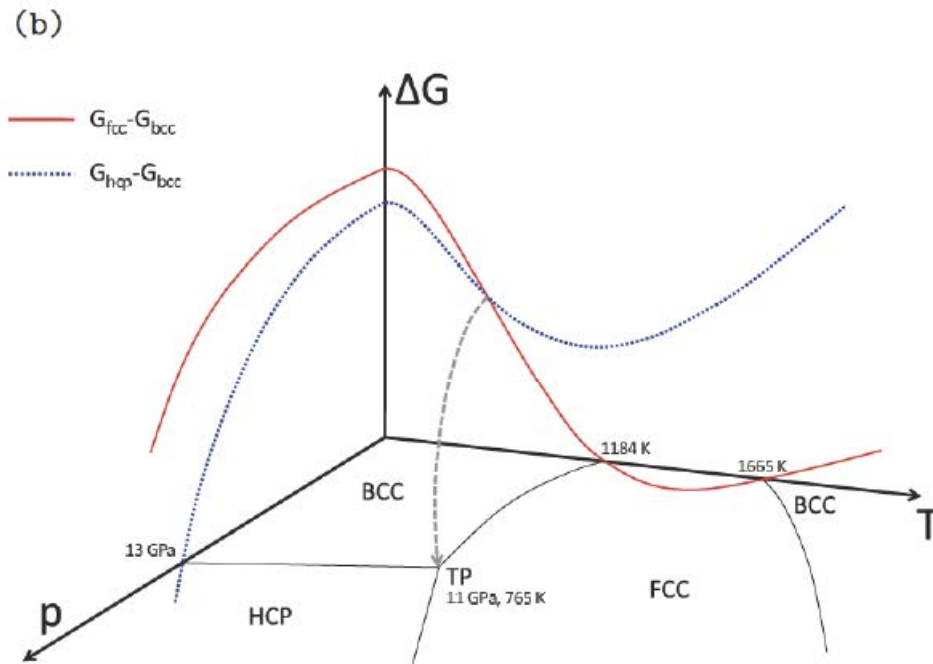
Our work on computational materials science at the atomic scale focuses on several challenges



The 'electron barrier: ' Fe polymorphism

T. Lee & S. Valone

MST-8 Materials Science and Technology

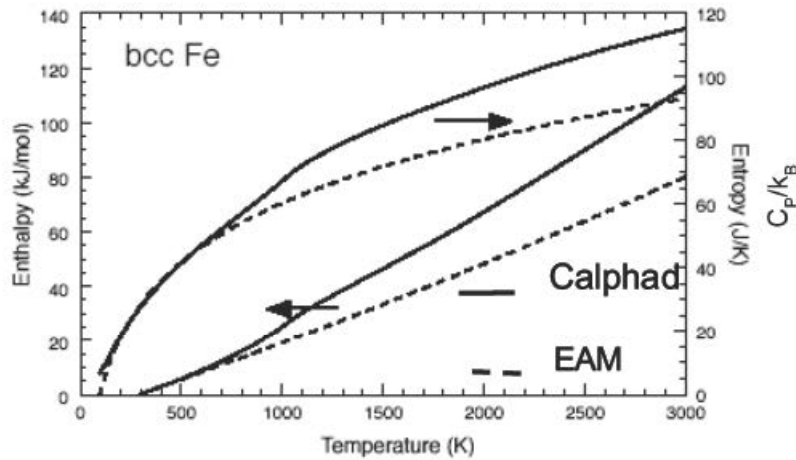


Fe has bcc-to-fcc transition as a function of T
 and a bcc-to-hcp transition as a function of P
 → a triple point

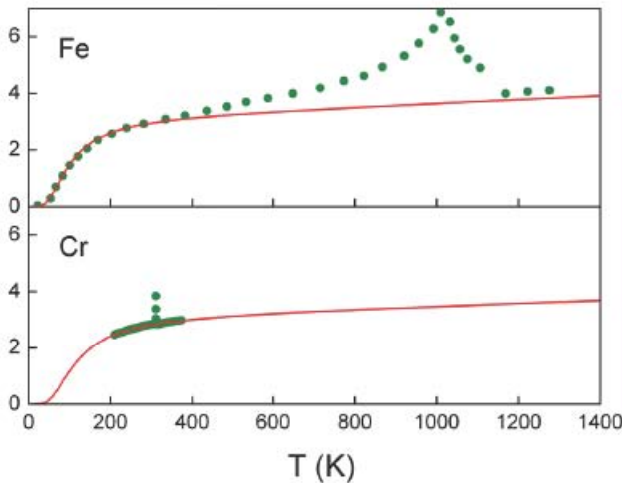
Classical potentials have so far been
 unable to capture both transitions
 simultaneously

Finite-T properties are difficult to capture when electronic effects are important

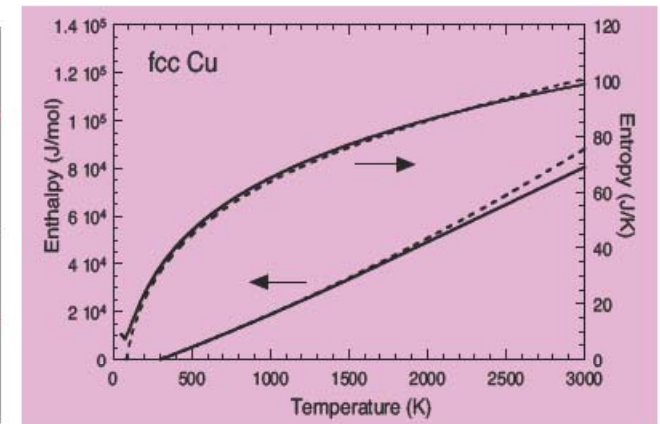
EAM and CALPHAD Fe enthalpies and entropies



Heat capacities of pure metals



Dots: experimental data
Lines: empirical potentials
From E. Martinez 2012

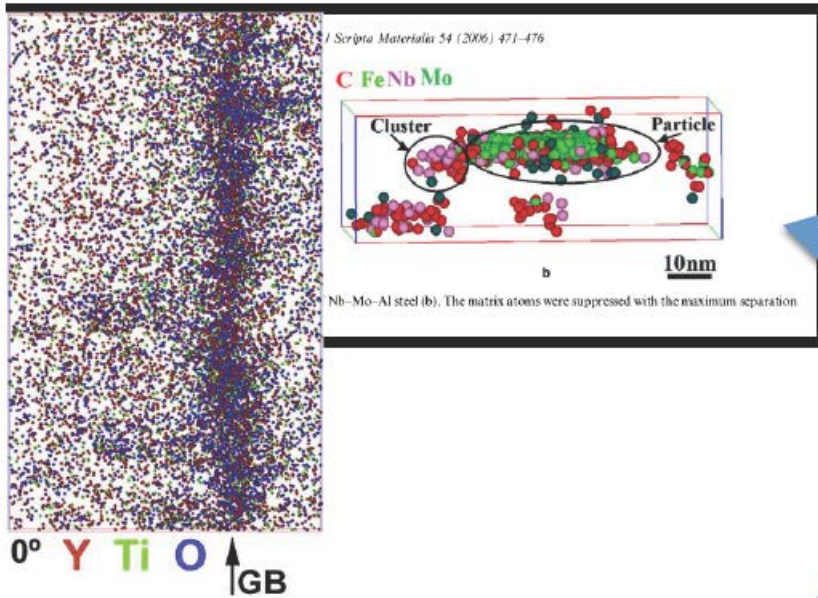


Cu, shown for comparison

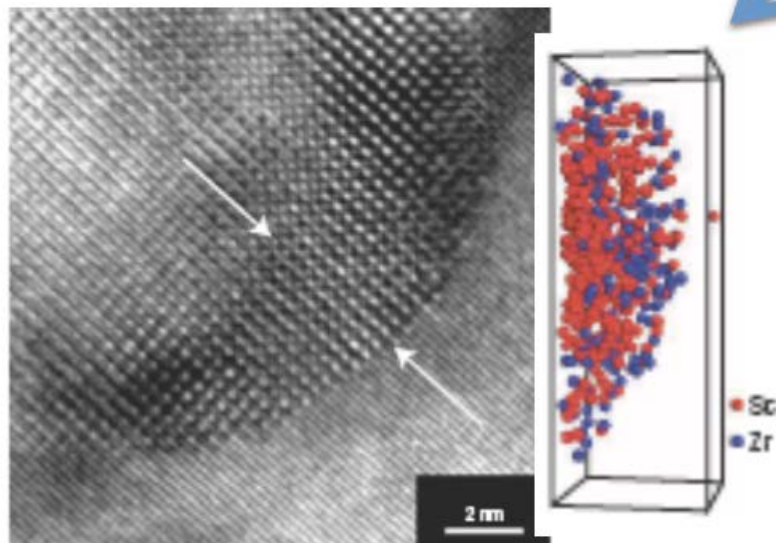
This behavior represents a major obstacle for empirical potentials for Fe, whose validity is therefore restricted to the FM phase, well below the Curie T

The 'thermal barrier'

ODS ferritic steels, Miller 2009



Al-Zr-Sc nanostructured alloy, Clouet 2006



Most of the nano-engineered materials today are

- non-equilibrium
- multiphase
- multicomponent

systems, where thermodynamics and kinetics play crucial roles in determining their microstructure

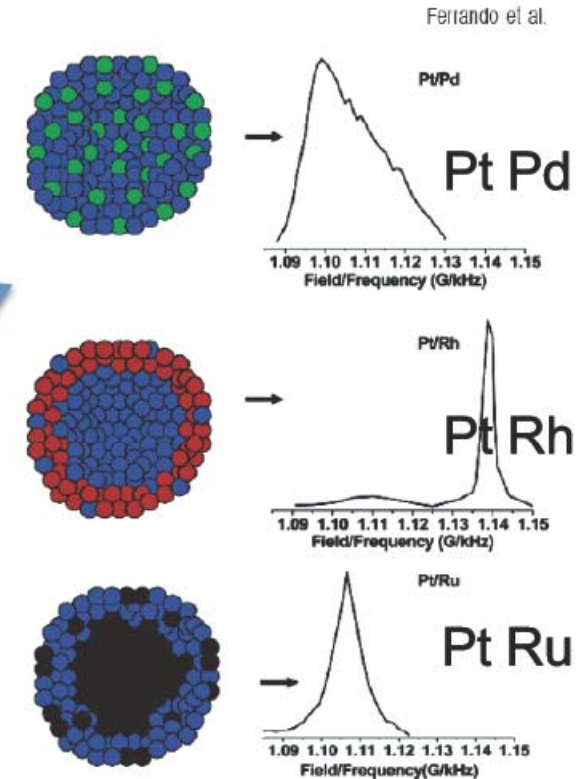


Figure 10. Schematic representation of three different Pt-alloy nanoparticle systems with their corresponding ^{195}Pt NMR spectra: (A) Pt-Pd, (B) Pt-Rh, and (C) Pt-Ru. Pt, Pd, Rh, and Ru atoms are shown in blue, green, red, and black, respectively. (Reprinted with permission from ref 129. Copyright 2003 American Chemical Society.)

Nanoalloys. Ferrando 2008

The 'thermal barrier'

Computational thermodynamics

Free energy G cannot be obtained as an ensemble average
 We use Mixed Hamiltonian with switching parameter λ

$$\lambda U + (1 - \lambda)W$$

Free energy F_W of the harmonic oscillator system can be computed analytically

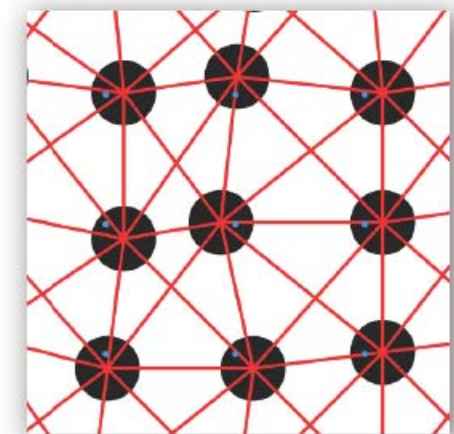
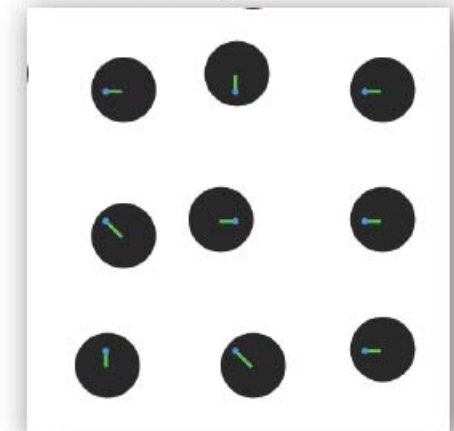
$$G_W = -kT \log \Omega_W \quad , \quad \Omega_W = \left(\frac{T}{T_{\text{Einstein}}} \right)^3$$

Evaluate the ensemble with respect to the pure Hamiltonians U (full interaction) and W (harmonic oscillators) and compute

$$G_U = G_W + \underbrace{\int_0^1 \langle U - W \rangle d\lambda}_{\text{switching work}}$$

We implemented this technique in LAMMPS (free distribution MD code)

Einstein Crystal



Fully interacting system

Other systems studied

MgLi

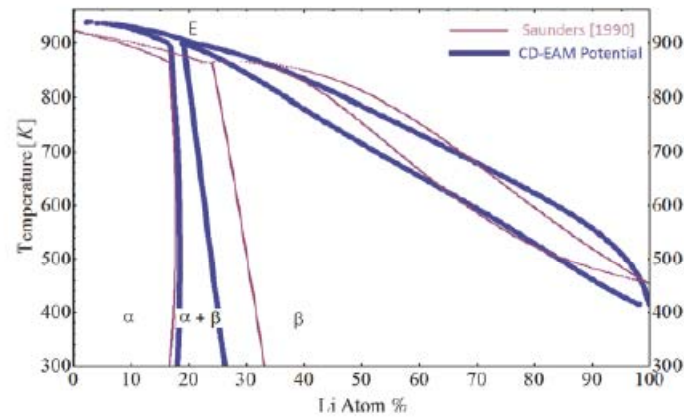


Figure 3: Phase diagram from the present work and Saunders [1990]. α represents hcp phase, β is bcc phase, $\alpha + \beta$ is two phase region, L is liquid region and E represents eutectic point.

COMPUTATIONAL MATERIALS SCIENCE 85 172-178 2014

CuNb

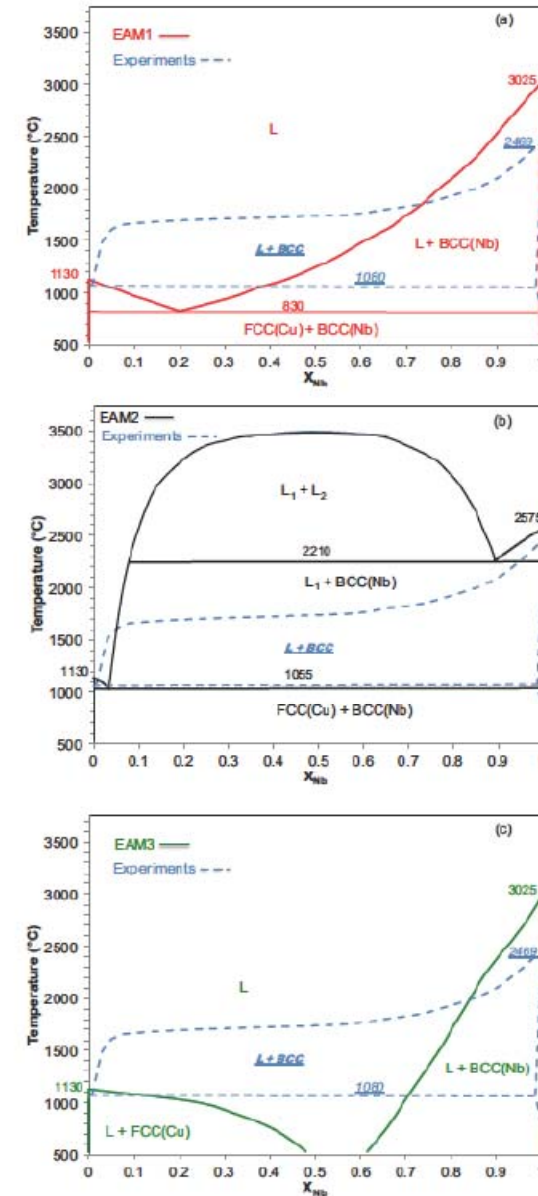


Figure 4. Equilibrium binary phase diagram computed using (a) EAM1, (b) EAM2 and (c) EAM3, compared with experimental phase diagram from [1]. The phase diagram from EAM1 shown in (a) is closest to the experimentally determined Cu-Nb phase diagram among all three potentials tested in this study.

Nucleation of α' in FeCr

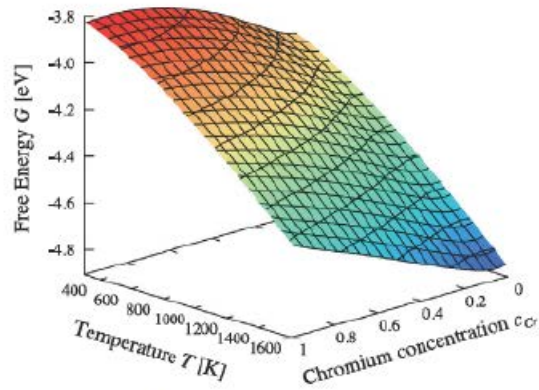


Fig. 1. Free energy surface $G(x,T)$.

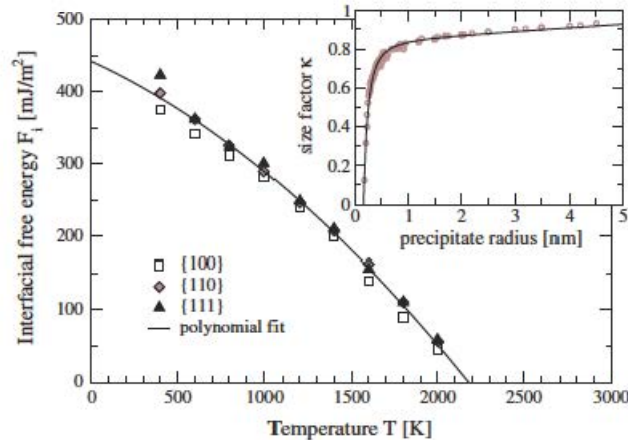


Fig. 2. Interfacial free energy of the FeCr system as a function temperature obtained by Sadigh and Erhart [6] using variance constrained semi grand canonical Monte Carlo simulations. The solid line shows the polynomial fit to the data used in our calculations. The inset shows the radius dependence of the interfacial energy normalized by the flat interface energy at 0 K.

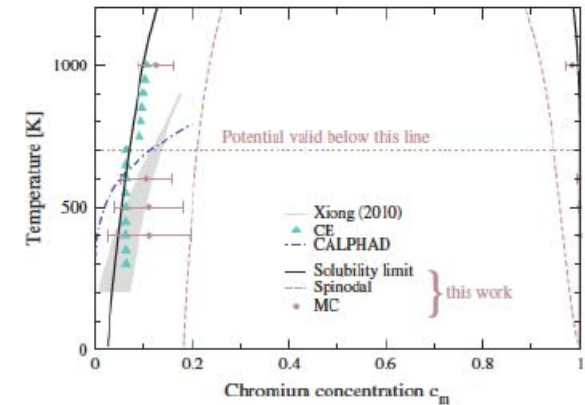


Fig. 3. Phasediagram of the FeCr system, calculated from the free energy surface. The solid curve marks the miscibility gap of the FeCr system, the dashed curve marks the spinodal line (the boundary of the thermodynamically unstable region). The diamond symbols with error bars show the solubility limits as obtained by a semi grand canonical Monte Carlo simulation. The shaded region gives a range of possible Cr solubility limits in Fe as obtained by Xiong et al. [3] while the triangles are results from cluster expansion (CE) calculations fitted to first principles data [17].

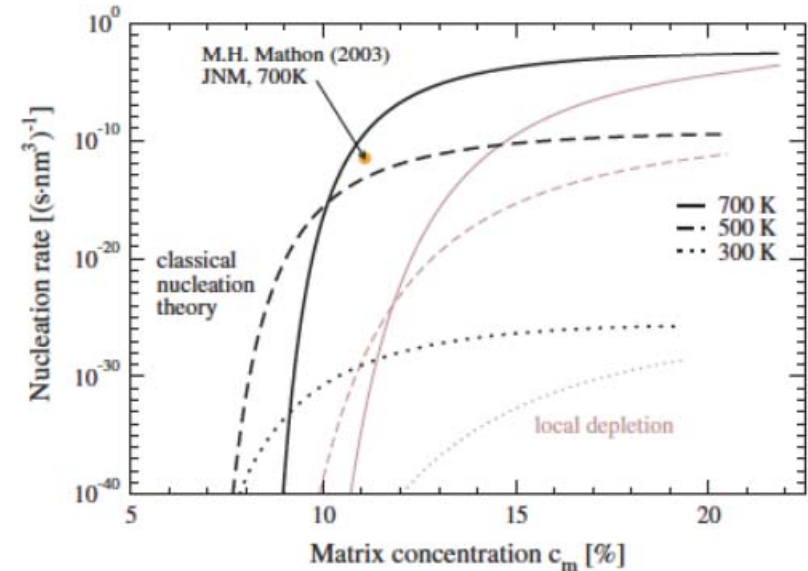


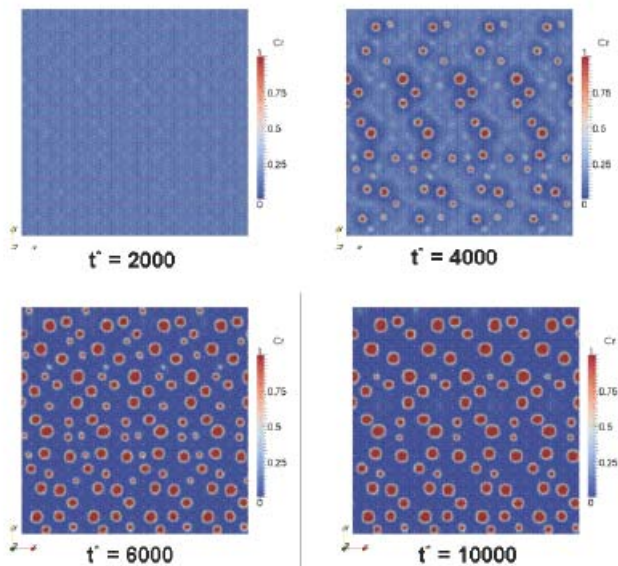
Fig. 6. Nucleation rates R per unit volume for the classical nucleation theory (black) and local depletion (gray) cases as a function of solute concentration in the matrix at 300 K, 500 K, and 700 K. A single experimental data point by Mathon et al. [20] on martensitic LA4Ta steel with 11.8% Cr at 700 K is shown in the top left.

Microstructural evolution of $\text{Fe}_{80}\text{Cr}_{20}$ at 535 K

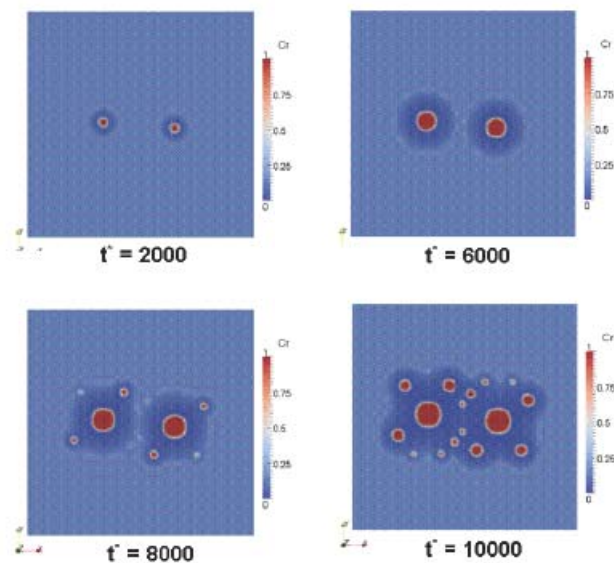
Work on Phase Field modeling by M. Tonks and P. Millet (INL) as part of the NEAMS program

Work on LKMC modeling done at LANL by E. Martinez in collaboration with CEA Saclay (Fr) as part of the EFRC program

In a single crystal



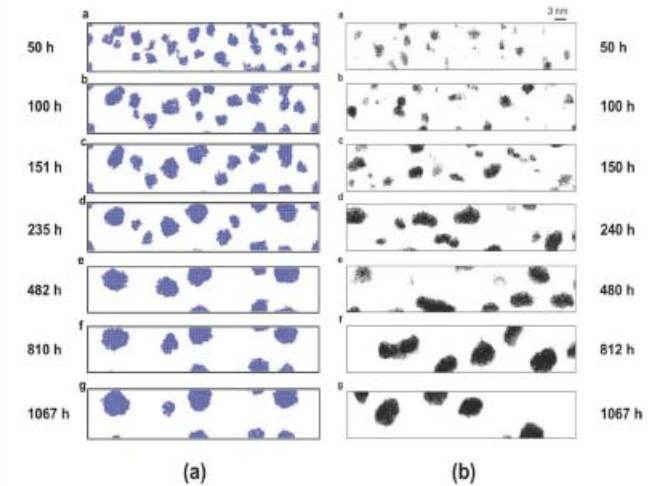
In presence of an edge dislocation dipole



LKMC

3D atom probe

Novy et al (2009)



The size / time barrier

Atomistic Kinetic Monte Carlo

Louis Vernon, Enrique Martinez, Blas Uberuaga, Art Voter, and Alfredo Caro
T and MST Divisions

Objective:

Many systems of interest share a common feature: their long-time dynamics consists of infrequent jumps between different states (i.e., activated processes).

Accelerated Molecular Dynamics methods (A. Voter's) and kinetic Monte Carlo (KMC) algorithms can be used to extend the simulated time.

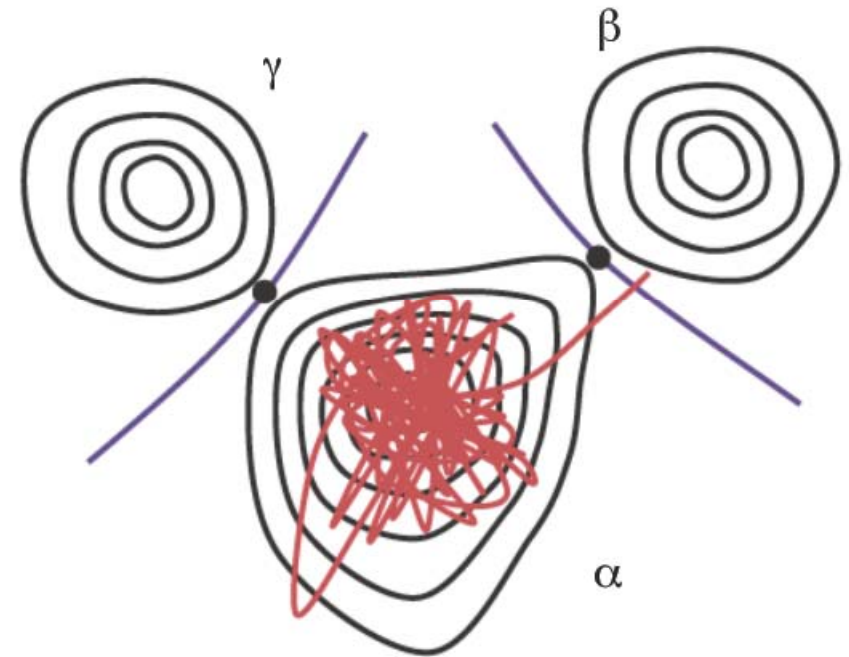
In this presentation we focus in the KMC algorithm

The MD timescale problem

Classical MD can only reach nanoseconds to microseconds due to the stiffness of the equations of motion (time step is limited to fs)

Processes of interest often take much longer:

- Vapor-deposited film growth (s)
- STM/AFM surface manipulation, nanoindentation (ms – s)
- Bulk and surface diffusion processes
- Radiation damage annealing (ns to years)
- Protein folding (μs - s)
- Precipitation

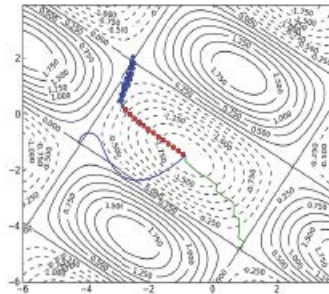


Our Kinetic Monte Carlo Approaches

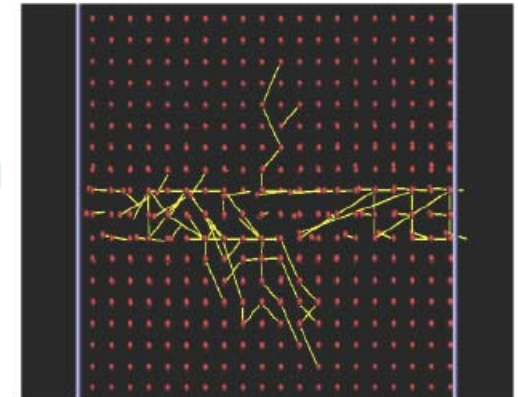
□ Self-learning KMC

- Dynamically explores the potential energy surface to discover all processes.
- Calculate the rates accurately.
- Is accurate and computationally demanding.

Transition searches on a distorted eggbox potential.



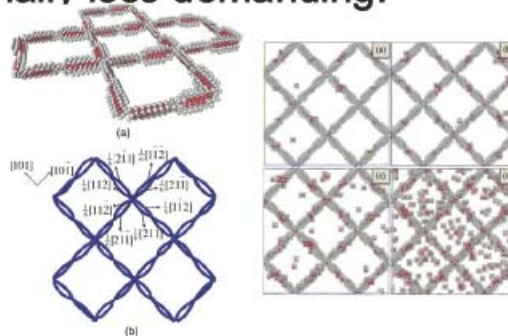
Defects diffuse to and within a complex grain boundary - evolved using SL-KMC.



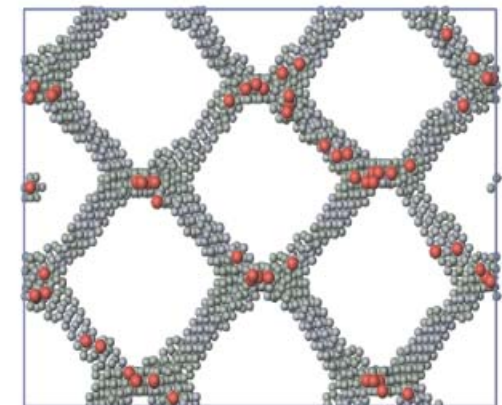
□ Event-driven KMC

- Uses the local microstructure to guess possible processes
- The accuracy in the rate calculation can be chosen
- Computationally less demanding.

Cluster of vacancies in a (100) twist boundary in Cu, showing the preference for vacancies to go to constrictions



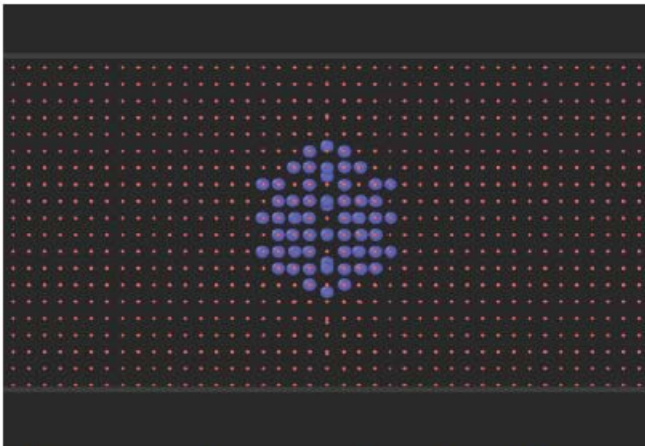
Clustering of vacancies at a (110) twist boundary in Fe, composed of a network of screw dislocations



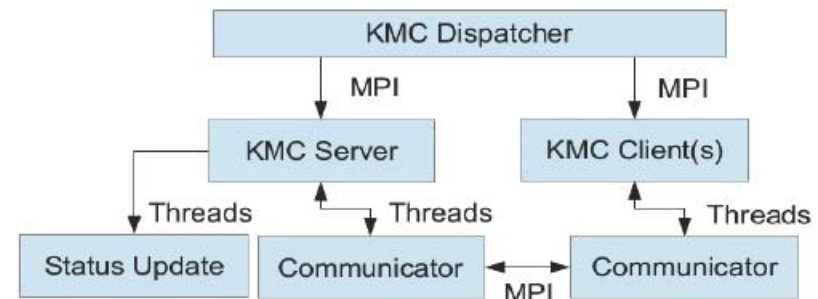
Self-Learning kinetic Monte Carlo

Transition searches are pricey

- Computationally more demanding than predefined processes.
 - Optimisation is essential.
 - Efficient transition searches.
 - Defect localisation.
 - Information recycling.
 - Parallelised workload.



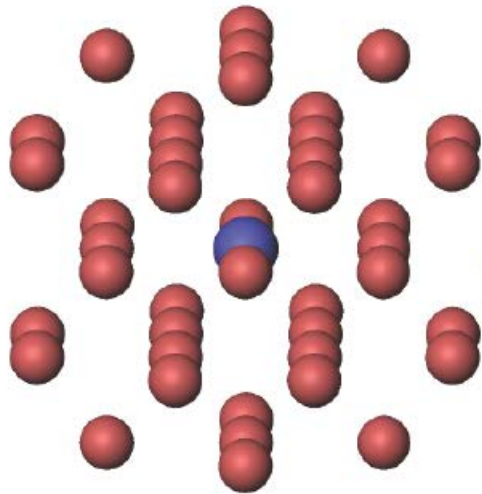
Transition searches are localised to regions containing defects.



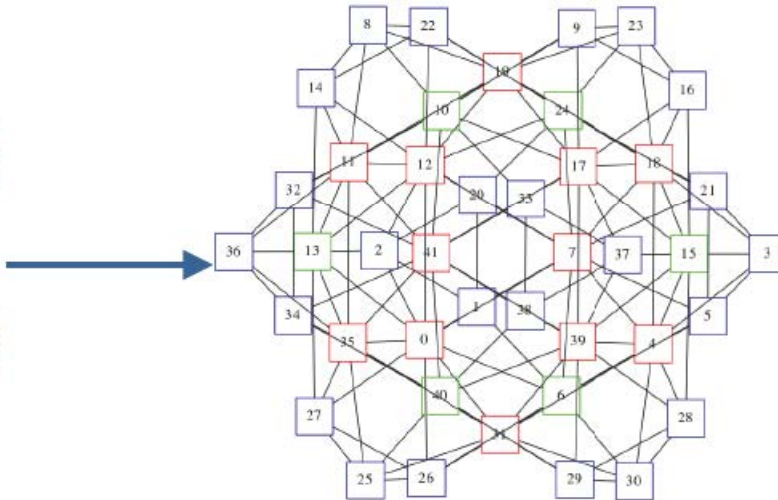
Transition searches and minimisations are distributed across many processors using MPI.

Localisation allows categorisation

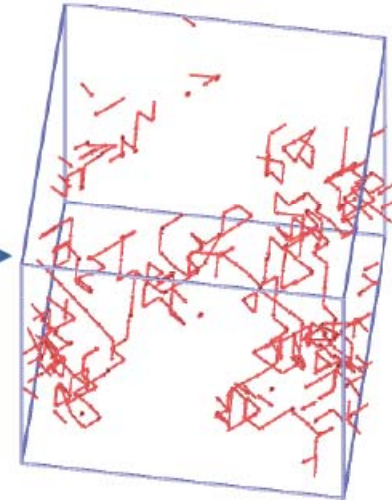
- Localising defects:
 - Reduced search dimensionality.
 - **Defect classification.**
 - Defect recognition.



Atoms local to a vacancy (highlighted) are extracted.



A connectivity graph/hash representation is determined.

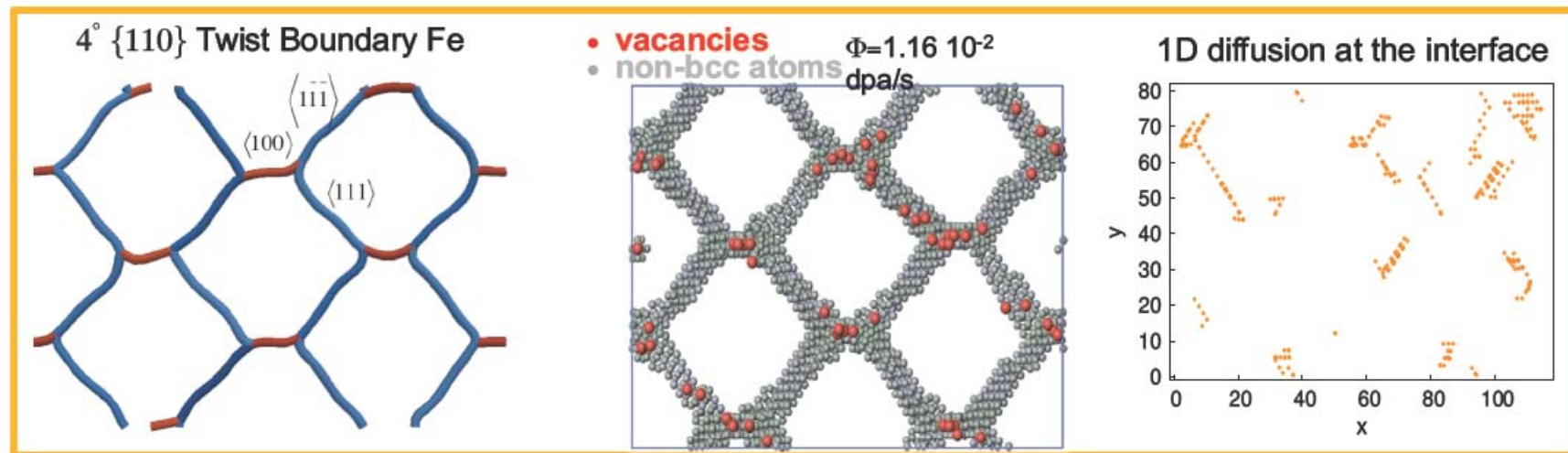


The vacancy rapidly diffuses with no new transition searches.

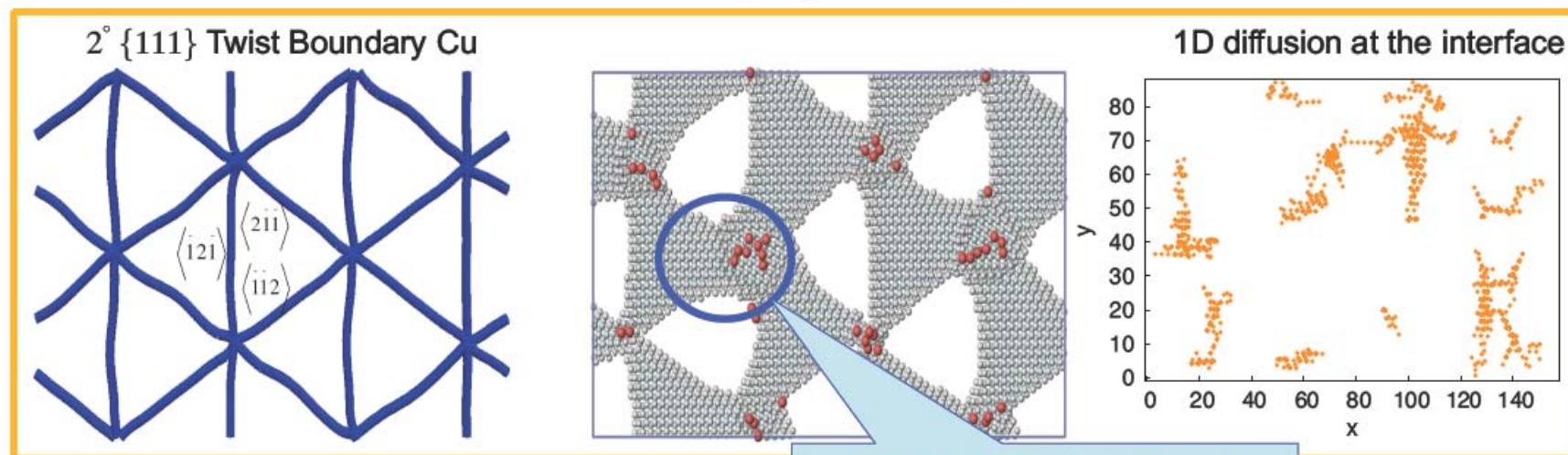
Transitions can be mapped onto equivalent defects

Event-Driven Kinetic Monte Carlo

Off-lattice Relaxations



$t = \sim 10^{-2}$ s, beyond MD capabilities



Dislocation rearrangement possible using Off-Lattice k-MC

Radiation effects on nanoscale metallic foams

Objective:

- Explore the physics of surface-driven bulk physical behavior, such as radiation tolerance

Opportunity:

- Nanoporous materials could become a new class of extremely radiation tolerant materials
 - Nanoporous materials offer a large amount of free surfaces
 - Free surfaces act as sinks providing opportunities for irradiation induced defects to annihilate through diffusion

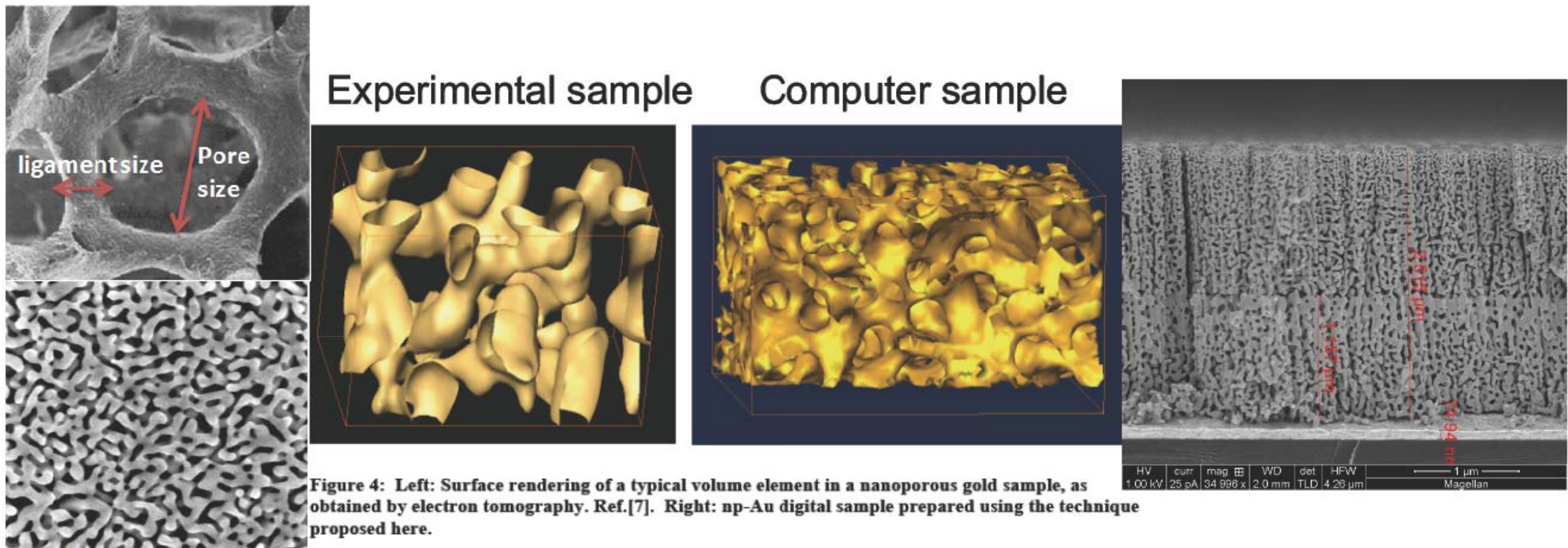
Cover of Nano Letters July 2012



Making foams in the computer

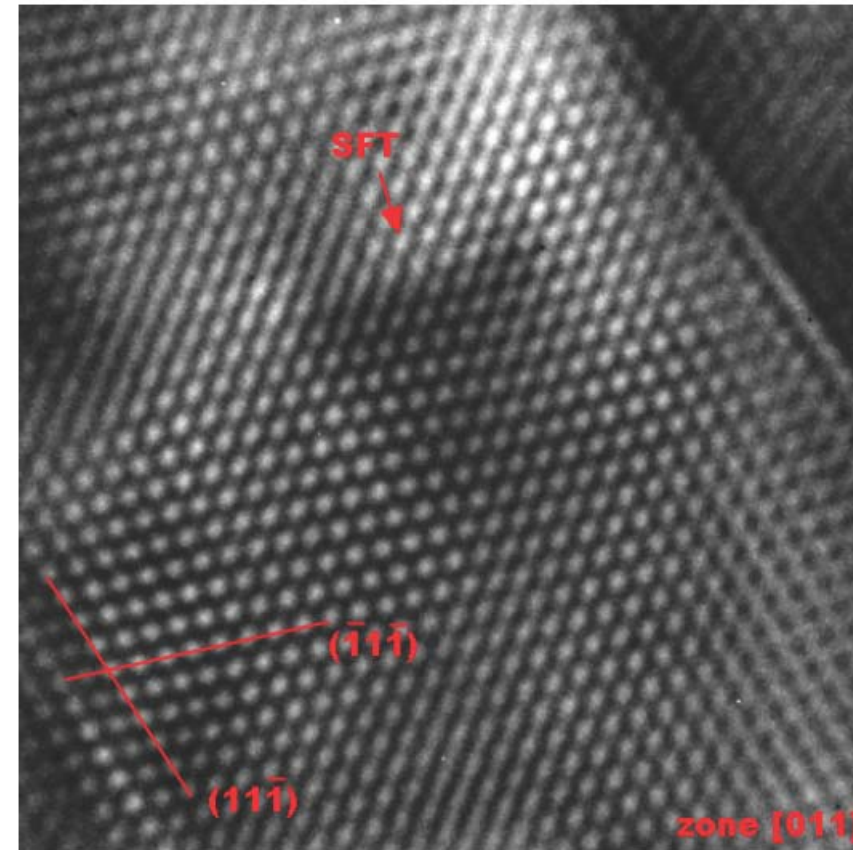
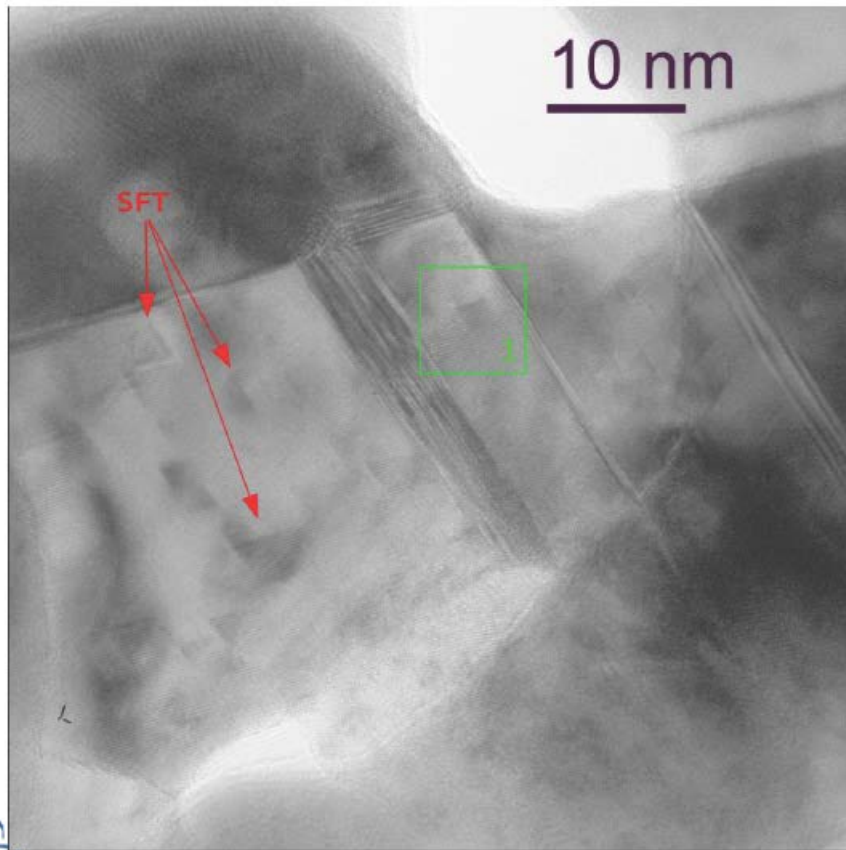
Two methods have been reported:

- Spinodal decomposition (an AB solution with a miscibility gap)
- Gas condensation (solidification of a low density gas)

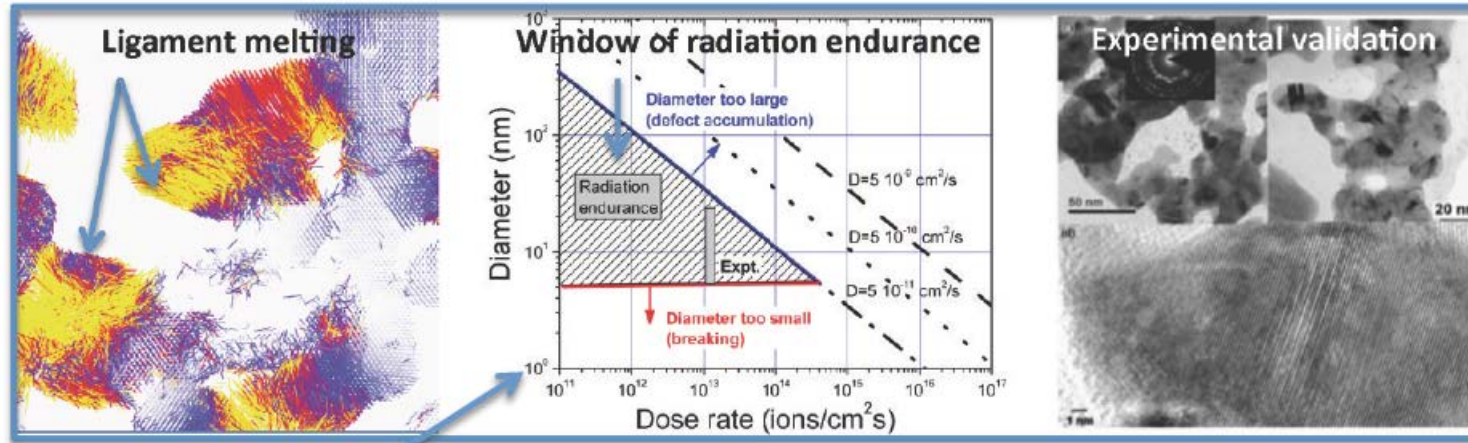


HRTEM shows SFTs are formed in irradiated np-Au

- SFTs are observed in np-Au foams irradiated at RT at intermediate and high flux values; i.e. flux $> 6 \times 10^{10}$ ions/cm²/s
- No SFTs observed at low dose-rates and/or LNT irradiations

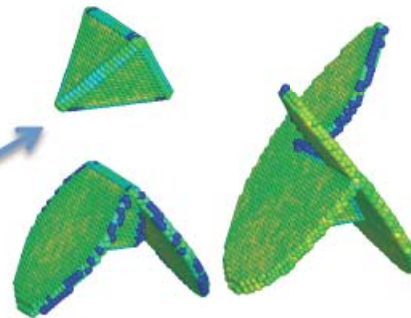


Are nanofoams radiation resistant?

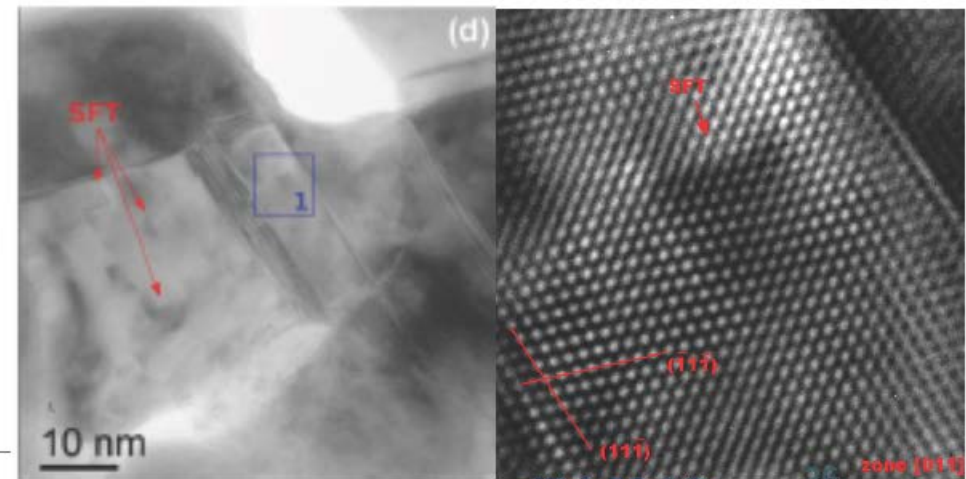
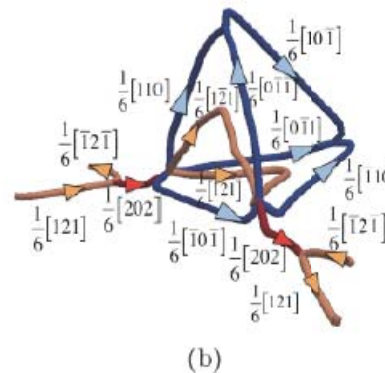
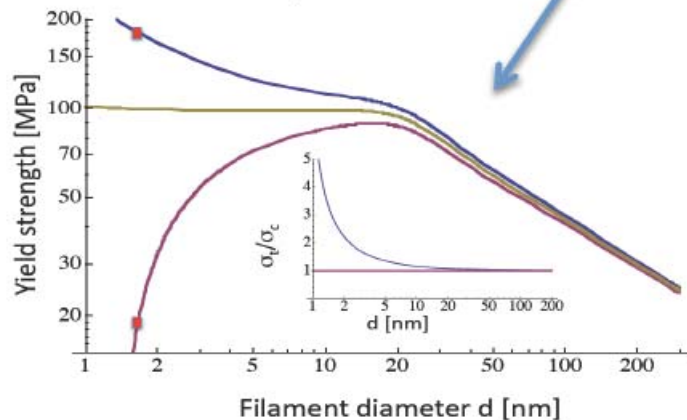


Major results:

- A window of radiation resistance
- Radiation produces little damage in nanoscale foams, due to the large surface to volume ratio
- Main damage mechanism is the creation of stacking fault tetrahedra, which induce a softening of the foam
- Strong a-symmetry in the mechanical response in tension and compression



Material synthesis at CINT, irradiations at IBL



Nanoscale He bubbles

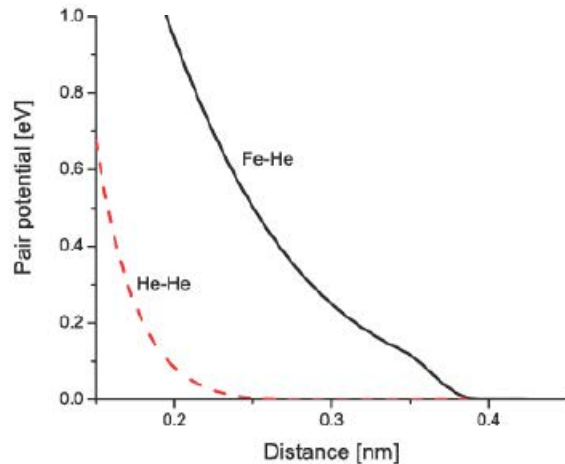
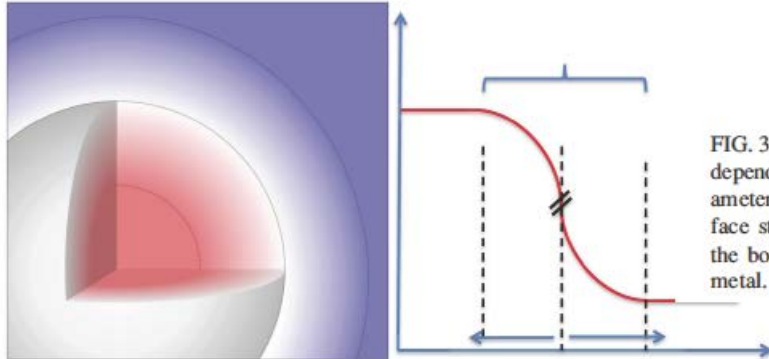


FIG. 1. Pair potentials for the He-He interaction from Ref. 21 and for He-Fe from Ref. 18. While the range of the He-He interaction can be considered nearest neighbors for the He densities of interest (~ 1 He/Vac), the range of the He-Fe goes well beyond that distance.

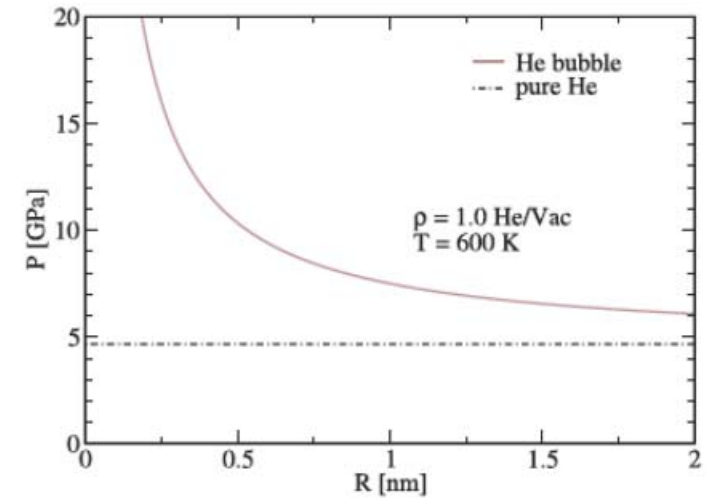


FIG. 5. Average pressure of a bubble of varying radius in the range 0–2 nm at density 1 He/Vac and $T = 600$ K. Also, in the figure the pressure of pure He at that density is indicated as a horizontal line. A significant deviation of pressure from the pure He EOS is apparent for bubbles below 2 nm in radius.

The interface width, determined by the metal-He interaction, dominates the properties of nanoscale bubbles, leading to the need of defining a new EOS for He in bubbles, that depends on bubble radius

Appl. Phys. Lett. 103, 213115 (2013)

Summary and Future Directions

Our computational materials science work is based on both,

- The use of well established techniques such as:
 - *Ab initio* electronic structure calculations to predict energetics of materials
 - Classical molecular dynamics
 - Computational thermodynamics
- The development of new models, algorithms, and tools to address problems such as:
 - The ‘electron barrier’
 - The ‘thermal barrier’
 - The ‘size / time barrier’

The research portfolio of our group on multiscale computational modeling is characterized by a significant effort on the development of new models, algorithms and tools at almost every scale in the multiscale paradigm, aiming at improving the current fidelity and accuracy limitations